

# Synthesis and Modeling of New Benzofuranone Histone Deacetylase Inhibitors that Stimulate Tumor Suppressor Gene Expression

Cédric Charrier,<sup>†</sup> Jonathan Clarhaut,<sup>‡</sup> Jean-Pierre Gesson,<sup>†</sup> Guillermina Estiu,<sup>§</sup> Olaf Wiest,<sup>§</sup> Joëlle Roche,<sup>‡</sup> and Philippe Bertrand<sup>\*,†</sup>

Laboratoire Synthèse et Réactivité des Substances Naturelles, Université de Poitiers, CNRS-UMR 6514, 40 Avenue du Recteur Pineau, Poitiers F-86022, France, Institut de Physiologie et de Biologie Cellulaires, Université de Poitiers, CNRS-UMR 6187, 40 Avenue du Recteur Pineau, Poitiers F-86022, France, Walther Cancer Research Center, Department of Chemistry and Biochemistry, University of Notre Dame, Notre Dame, Indiana 46556-5670

Received January 21, 2009

New benzofuranones were synthesized and evaluated toward NCI-H661 non-small cell lung cancer cells. Benzamide derivatives possessed micromolar antiproliferative and histone deacetylase inhibitory activities and modulate histone H4 acetylation. Hydroxamic acids were found to be potent nanomolar antiproliferative agents and HDAC inhibitors. Computational analysis presented a rationale for the activities of the hydroxamate derivatives. Impact of the HDAC inhibition on the expression of E-cadherin and the SEMA3F tumor suppressor genes revealed new promising compounds for lung cancer treatments.

## Introduction

Chemical modifications of DNA and histones are eukaryotic cellular events modulating DNA transcription and responsible for altered epigenetic modifications during cancer progression.<sup>1</sup> Histone modifications control chromatin remodeling, with acetylation giving the inactive chromatin and DNA transcription repression. The acetylation and deacetylation of histones are mediated by histone acetyl transferases and histone deacetylases (HDAC<sup>a</sup>).<sup>2</sup> Overexpression of HDAC has been reported in cancers, and development of HDAC inhibitors (HDACi) is a promising anticancer strategy.<sup>3</sup> HDACi were isolated (trichostatin A (TSA) (**1**), apicidin (**4**), Chart 1) or synthesized, like SAHA (**2**), FDA approved for treating cutaneous T-cell lymphoma,<sup>4</sup> or benzamide MS-275 (**3**). The most important HDACi are the hydroxamic acids group (**1**, **2**), followed by the benzamides (**3**), the cyclic tetrapeptides (**4**), the carboxylic acids, and the electrophilic ketones.

HDACi have a functional group, binding the zinc atom of the active site, linked to a cap moiety by a spacer fitting the geometry of the active site channel of HDAC. The cap can produce specific interactions with the external surface of the protein, leading to HDACi selectivity.<sup>5</sup> In the protein p53, the acetylated K<sup>382</sup> amino group is close to the external Tyr100 and Asp101 HDAC8 residues and stabilized by hydrogen bonding contacts between the NH backbone of the substrate and the Asp101.<sup>6</sup> These pairs of residues conserved in classes I/II/IV<sup>7</sup> were suggested to be important for selectivity.

Benzamides are more active on class I,<sup>8</sup> tetrapeptide **4** is more active on HDAC2,3, and several alkylthiols are selective HDAC8 inhibitors.<sup>9</sup> Hydroxamic acids are nonselective. SAHA is an inhibitor of most members of the class I/II but is a poor HDAC8 ligand. HDAC6 selectivity can result from preferred

interactions of large and lipophilic caps with residues sitting outside the entry of the active site channel<sup>10</sup> as in tubacin (**5**). These interactions cannot be established in the class I isoforms. Molecular modeling explained the mutation effects of key residues of the channel<sup>11</sup> and the selectivity of thiophenyl-biaryl binders in HDAC1 vs HDAC3.

From our previous work on TSA analogues, we planned to produce more potent HDACi by replacing the methylene bridge in compound **6b**<sup>12a</sup> (Scheme 1) by an isosteric oxygen atom, leading to a new family of compounds **7** with possible better biological activities and selectivity for HDAC1 vs HDAC6.<sup>12</sup> Representative ligands were modeled in homology models of HDAC1 and HDAC6.<sup>10b</sup> The expression of E-cadherin and the semaphorin 3F (SEMA3F) tumor suppressor gene, two known HDACi targets in lung cancer, were evaluated. E-Cadherin plays a major role in epithelial cell adhesion, and down regulation is involved in several tumor progression mechanisms<sup>13</sup> and correlated to poor prognosis in lung cancer. SEMA3F is expressed by multiple cell types, modulating the tumor angiogenesis and progression.<sup>14</sup> SEMA3F expression is lost or reduced in lung cancers. Restoring SEMA3F and E-cadherin expression could be a therapeutic strategy in lung cancer.

## Results and Discussion

Analogues **7** were prepared from furanones **13** (Scheme 1).<sup>12</sup> Acid **8** gave the phenol **10b** by esterification and *N,N*-dimethylation. Etherification of phenols **10** afforded ethers **12**, cyclized in situ to the esters **14**, heated to afford on decarboxylation furanones **13**. The decarboxylation of **14a** was completed by an additional stirring with HCl 6 N. Benzofuranones **13** were reacted with **15** to give aldehydes **16**. The unsuccessful initial procedure was modified to use NaOMe/MeOH as a base.<sup>12</sup>

Acids **19** were obtained in good yields by a two-step procedure from aldehydes **16**.<sup>12a</sup> Hydroxamic acids **7a,b** were prepared by reacting acids **19** with the *O*-tetrahydropyranyl protected hydroxylamine, followed by acidic methanolysis. Coupling of acids **19** with 1,2-diaminobenzene gave the benzamides **7c,d**.

Antiproliferative activities were evaluated against NCI-H661 non-small cell lung cancer cells (Figure S1 and Table 1, Supporting Information). Compound **1** gave a 100 nM IC<sub>50</sub>

\* To whom correspondence should be addressed. Phone: (33) 05 49 45 41 92. Fax: (33) 05 49 45 37 02. E-mail: philippe.bertrand@univ-poitiers.fr.

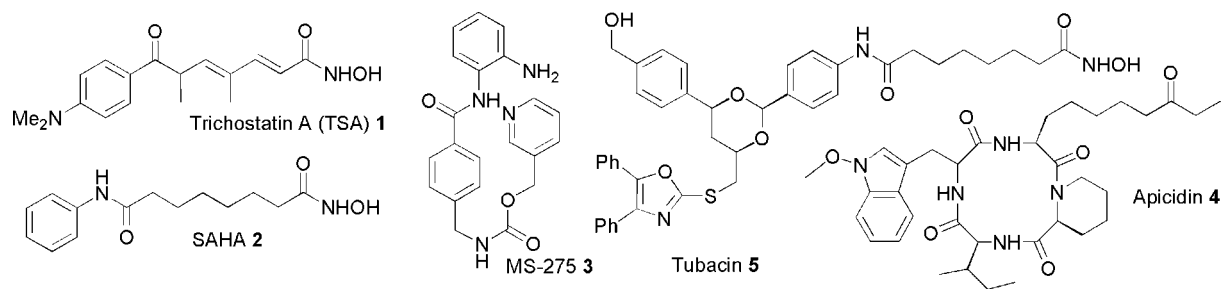
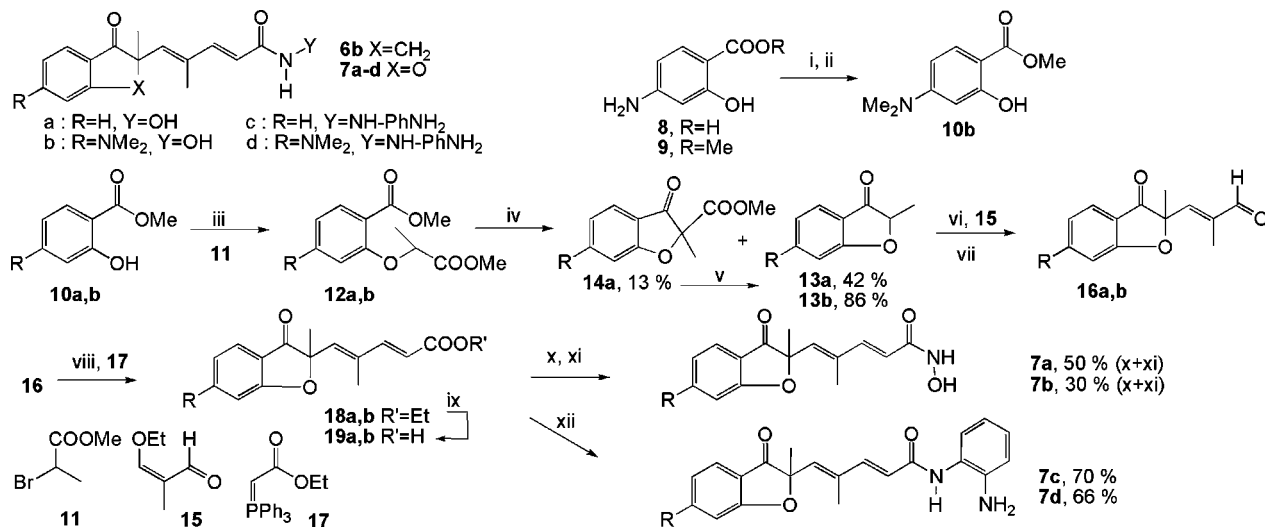
<sup>†</sup> Laboratoire Synthèse et Réactivité des Substances Naturelles, Université de Poitiers.

<sup>‡</sup> Institut de Physiologie et de Biologie Cellulaires, Université de Poitiers.

<sup>§</sup> Walther Cancer Research Center, Department of Chemistry and Biochemistry, University of Notre Dame.

<sup>a</sup> Abbreviations: HDAC, histone deacetylases; HDACi, HDAC inhibitors; SEMA3F, semaphorin 3F; MD, molecular dynamics.

## Chart 1. Examples of HDAC Inhibitors

Scheme 1. Preparation of Benzofuranones<sup>a</sup>

<sup>a</sup> Reagents: (i) H<sub>2</sub>SO<sub>4</sub>, MeOH, 54%; (ii) CH<sub>2</sub>O, NaBH<sub>3</sub>CN, 65%; (iii) **11**, K<sub>2</sub>CO<sub>3</sub>, DMF, 20 °C, overnight; (iv) K<sub>2</sub>CO<sub>3</sub>, DMF, reflux, 4 h; (v) HCl 6 N, DMF, 4 h; (vi) MeONa, MeOH, **15**, reflux; (vii) HCl 6 N, AcOEt, 80–81%; (viii) PhH, reflux, **17**, 85%; (ix) LiOH aq, THF:MeOH, 95%; (x) H<sub>2</sub>N-OTHP, TBTU, DMF, NEt<sub>3</sub>; (xi) Amberlyst resin H<sup>+</sup>, CH<sub>2</sub>Cl<sub>2</sub>, MeOH; (xii) H<sub>2</sub>N-Ph-NH<sub>2</sub>, EDC, THF.

value. Compound **7a** was found less active (IC<sub>50</sub> of 1 μM) and **7b** more potent (IC<sub>50</sub> of 45 nM). The benzamides **7c,d** were active at higher doses (IC<sub>50</sub> 3 and 4 μM, respectively), in agreement with previous data.<sup>8,12</sup> The HDAC inhibition was analyzed for histone H4 and tubulin acetylation (Figure 1A).<sup>12</sup> At 300 nM, **1** and **7b** similarly induced histone H4 and tubulin acetylation. Interestingly, **7a** at 300 nM induced only tubulin acetylation, while strong HDAC inhibition appeared at 3 μM for histone H4 acetylation. In contrast, benzamide derivatives **7c,d** were inactive at 300 nM and a moderate HDAC inhibition was observed at 3 μM on histone H4 acetylation. We tested E-cadherin and SEMA3F expressions by quantitative real-time RT-PCR (Figure 1B). As expected, **1** (300 nM) stimulated E-cadherin and SEMA3F expression, increasing their mRNA levels of about 50- and 4-fold, respectively. The same efficiency was obtained with **7b** (300 nM). A 3 μM concentration was necessary for **7a** to reach the level of stimulation of TSA and **7b**. Again, the benzamide derivatives were efficient only at 3 μM, without reaching the efficiency of **1** and **7b**.

The most active compounds **6b** and **7b** were selected for computational studies. The role of the oxygen bridge and the spatial position of the dimethylamino group, shown to improve the HDACi activities,<sup>12</sup> were evaluated. In compounds **6** and **7**, only the free rotating bond connecting the ketone rings to the diene chain was expected to play a role in the resulting conformations. In this respect, we selected only one stereoisomer to perform molecular dynamics (MD) simulations. Compounds **6b** and **7b** bound to HDAC1 and HDAC6 were analyzed using MD protocol to capture any specific interaction of the protein

with the oxygen atom of the benzofuranone moiety that may explain the observed HDACi activities of compound **7b**. In the two isoforms, the hydroxamic group is bonded to the zinc ion and the hydrocarbon chain (linker region) fills the narrow portion of the pocket lined by hydrophobic groups (Phe205 and Phe150 in HDAC1). Compounds **6b** and **7b** in HDAC1 showed no preferential orientation of the cap (Figure S2, Supporting Information). The same orientation is favored at the end of the dynamics for both ligands, which is only kept by lipophilic interactions with Phe150 and the residues of a proline-rich lipophilic pocket (Figure 2A). Similar interactions were found for **6b** and **7b** in HDAC6, where Pro698 replaces Arg270 (Figure 2B), and proline residues also defined a lipophilic pocket.

These results confirmed the low impact of the C2 stereochemistry.

## Conclusion

In conclusion, the synthesis of new TSA analogues is described, with antiproliferative activities and HDACi properties. The hydroxamates **7a,b** were found active on histone H4 and tubulin acetylation, suggesting a class I/II inhibitory activity. Compound **7b** confirmed the key role of the dimethylamino group for activity. Our benzamides **7c,d** were found more potent on class I HDAC at micromolar concentrations. The HDAC inhibition was correlated with upregulation of two tumor suppressor genes, SEMA3F and E-cadherin, demonstrating potential therapeutic application for lung cancers. MD simulations of **6b** and **7b** confirmed the interaction of the dimethyl-

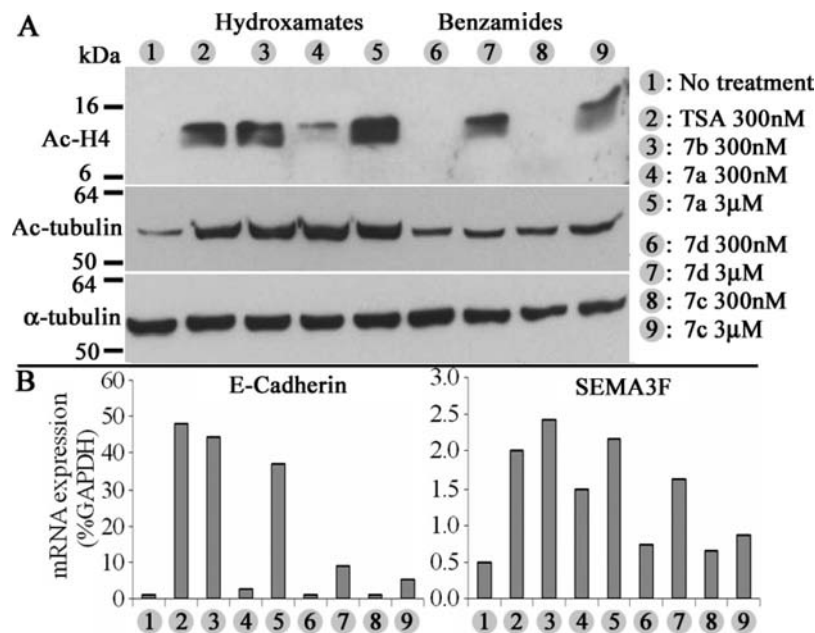


**Figure 1.** (A) Analysis of histone H4 and tubulin acetylation. NCI-H661 cells were treated for 6 h with compounds **1** and **7a–d**. Western blots represent three independent experiments. Left: kDa, molecular weights; Ac-H4, acetylated histone H4; Ac-tubulin, acetylated tubulin.  $\alpha$ -Tubulin: loading control. (B) E-Cadherin (left) and SEMA3F (right) mRNA levels. Values obtained from duplicates are expressed in % of GAPDH expression.

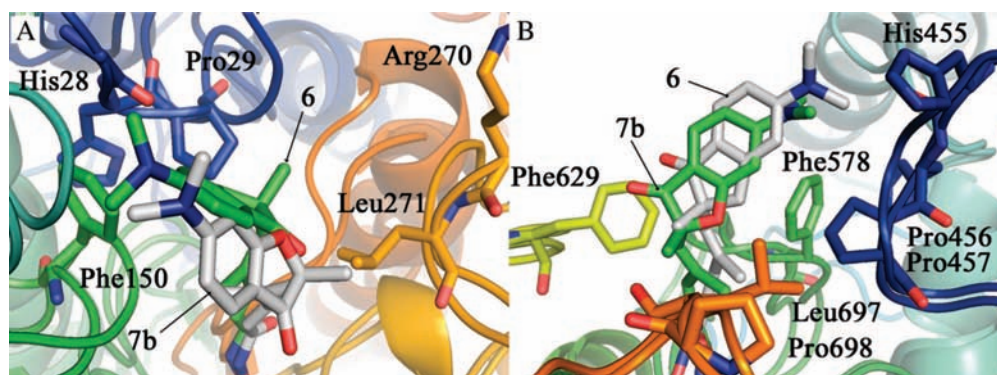


**Figure 2.** Stick representations of the interactions of compounds **6b** and **7b** with residues lining the active site pocket of HDAC1 (A) and HDAC6 (B).

lamino moiety with the surface of the protein as well as several hydrophobic contacts of the dihydrofuran ring at the entry of the active site. The cap region does not have a preferred orientation and rotates over the course of the simulation as found for SAHA<sup>10b</sup> and typical for hydrophobic interactions. Comparison with the results found for tubacin analogues<sup>10b</sup> indicated the potential for further development of isoform selectivity by chemical modification of these regions. Work is in progress to develop more hindered compounds as potential selective HDACi.

## Experimental Section

General methods and analytical HPLC conditions, syntheses of known compounds, and access to benzofuranones intermediates **13a–b**, **16a–b**, **18a–b**, and **19a–b** are reported in Supporting Information. Compounds used for biological tests were at least 95% pure as determined by HPLC methods (see Supporting Information).

**5-(2-Methyl-3-oxo-2,3-dihydro-benzofuran-2-yl)-4-methyl-penta-2,4-dienoic Acid Hydroxamide (7a).** To a solution of acid **19a** (155 mg, 0.6 mmol) in DMF (2 mL) were added TBTU (288 mg, 0.9 mmol) and  $\text{NEt}_3$  (0.165 mL, 1.2 mmol). After 2 h,  $\text{NH}_2\text{-OTHP}$  was added (106 mg, 0.9 mmol) and stirring continued

overnight. The solution was neutralized with saturated  $\text{NaHCO}_3$  and extracted with  $3 \times 50$  mL EtOAc. The combined organic layers were dried ( $\text{MgSO}_4$ ) and concentrated under vacuum. The protected OTHP derivative was purified (flash chromatography on silica, PE: EtOAc 60:40) and dissolved in 5 mL of MeOH. Then 150 mg of Amberlyst were added and stirring at ambient temperature continued 3–6 h until the starting material was consumed. The resin was filtered off and MeOH removed under vacuum. Purification (flash chromatography on silica, EtOAc) was followed by recrystallization in a refrigerator from PE:EtOAc to give **7a** as a yellow solid (82 mg, 50%).  $^1\text{H}$  NMR (300 MHz;  $\text{CD}_3\text{OD}$ )  $\delta$  ppm: 1.6 (s, 3H), 1.8 (s, 3H), 5.8 (d, 1H,  $J = 15.4$  Hz), 5.94 (s, 1H), 6.85–7.3 (m, 2H), 7.6 (m, 2H),  $^{13}\text{C}$  NMR (75 MHz;  $\text{CD}_3\text{OD}$ )  $\delta$  ppm: 14.1, 23.8, 88.8, 113.5, 116.6, 119.3, 122.1, 124.9, 134.8, 138.3, 138.4, 145.5, 171.0, 202.0. HRMS ESI:  $(\text{M} + \text{H})^+(\text{C}_{15}\text{H}_{16}\text{NO}_4)$ : calcd 274.10793, found 274.1084.

**5-(6-Dimethylamino-2-methyl-3-oxo-2,3-dihydro-benzofuran-2-yl)-4-methyl-penta-2,4-dienoic Acid Hydroxamide (7b).** Prepared as above from acid **19b** (188 mg, 0.625 mmol), DMF (2 mL), TBTU (300 mg, 0.937 mmol), and  $\text{NEt}_3$  (0.17 mL, 1.25 mmol). Recrystallization from PE:EtOAc in a refrigerator gave **7b** as a light-pink solid (60 mg, 30%, mp 131–132 °C).  $^1\text{H}$  NMR (300 MHz;  $\text{CD}_3\text{OD}$ )  $\delta$  ppm: 1.45 (s, 3H), 1.9 (s, 3H), 3.1 (s, 6H),



5.8 (s, 1H), 5.80 (d, 1H,  $J = 15.6$  Hz), 6.16 (d, 1H,  $J = 2.1$  Hz), 6.45 (dd, 1H,  $J = 2.1, 8.9$  Hz), 7.05 (d, 1H,  $J = 15.6$  Hz), 7.30 (d, 1H,  $J = 8.9$  Hz).  $^{13}\text{C}$  NMR (75 MHz;  $\text{CD}_3\text{OD}$ )  $\delta$  ppm: 14.0, 25.0, 41.0, 90.8, 93.5, 108.5, 110.3, 119.1, 126.9, 136.9, 138.6, 146.1, 160.4, 166.6, 175.2, 200.7. IR neat: 3200, 2900, 1600, 1532, 1352, 1119. HRMS ESI:  $(\text{M} + \text{Na})^+$   $\text{C}_{17}\text{H}_{20}\text{N}_2\text{O}_4\text{Na}$  calcd 339.13208, found 339.1320;  $(\text{M} + \text{H})^+$   $\text{C}_{17}\text{H}_{21}\text{N}_2\text{O}_4$  calcd 317.15013, found 317.1510.

**5-(2-Methyl-3-oxo-2,3-dihydro-benzofuran-2-yl)-4-methyl-penta-2,4-dienoic Acid Benzamide (7c).** To a solution of acid **19a** (134 mg, 0.52 mmol) in dry THF (5 mL) was added 1,2-diaminobenzene (340 mg, 3.12 mmol) and EDC (145 mg, 0.68 mmol). After stirring overnight, the solution was concentrated under vacuum. EtOAc was added (50 mL), and the resulting organic layer was washed with  $\text{H}_2\text{O}$  (30 mL) and then twice with aq 1 N NaOH (20 mL). The organic layer was dried ( $\text{MgSO}_4$ ) and solvents removed under vacuum. The resulting solid was purified (flash chromatography EtOAc:PE 50:50) to give **7c** as a pale-yellow powder (127 mg, 70%, mp 174–175 °C).  $R_f$ : 0.8 (EtOAc:PE 50:50).  $^1\text{H}$  NMR (300 MHz;  $\text{CDCl}_3$ )  $\delta$  ppm: 1.60 (s, 3H), 1.90 (s, 3H), 3.95 (s, 2H), 5.90 (s, 1H), 6.10 (d, 1H,  $J = 15.3$  Hz), 6.75 (m, 1H), 7.1 (m, 4H), 7.25 (d, 1H,  $J = 15.3$  Hz), 7.6 (m, 3H).  $^{13}\text{C}$  NMR (75 MHz;  $\text{CDCl}_3$ )  $\delta$  ppm: 13.7, 23.9, 88.8, 113.5, 118.1, 119.3, 119.4, 120.8, 122.1, 124.3, 124.9, 125.1, 127.1, 134.8, 137.3, 138.4, 140.7, 145.9, 164.3, 170.9, 201.8. IR neat: 3200, 2900, 1715, 1610, 1460, 1300, 1186. HRMS ESI:  $(\text{M} + \text{Na})^+$  calcd 371.13716, found 371.1378.

**5-(6-Dimethylamino-2-methyl-3-oxo-2,3-dihydro-benzofuran-2-yl)-4-methyl-penta-2,4-dienoic Acid Benzamide (7d).** Prepared as above from acid **19b** (157 mg, 0.52 mmol), THF (5 mL), 1,2-diaminobenzene (340 mg, 3.12 mmol), and EDC (145 mg, 0.68 mmol). Purification (flash chromatography EtOAc:PE 60:40) gave **7d** as a pale-yellow powder (134 mg, 66%, mp: 136–140 °C).  $R_f$ : 0.8 (EtOAc:PE 60:40).  $^1\text{H}$  NMR (300 MHz;  $\text{CDCl}_3$ )  $\delta$  ppm: 1.6 (s, 3H), 1.9 (s, 3H), 3.1 (s, 6H), 3.6 (s, 2H), 5.9 (s, 1H), 6.0 (d, 1H,  $J = 15.2$  Hz), 6.16 (s, 1H), 6.42 (dd, 1H,  $J = 2.1, 8.9$  Hz), 6.7 (m, 2H), 7.0 (t, 1H,  $J = 7.5$  Hz), 7.2 (m, 2H), 7.60 (d, 1H,  $J = 8.8$  Hz), 7.9 (s, 1H).  $^{13}\text{C}$  NMR (75 MHz;  $\text{CDCl}_3$ )  $\delta$  ppm: 13.6, 24.3, 40.5, 89.4, 92.4, 107.7, 108.1, 116.7, 118.1, 119.3, 120.5, 124.5, 125.2, 125.9, 127.0, 136.1, 136.7, 140.8, 146.3, 157.9, 164.6, 173.2, 198.3. IR neat: 3249, 2900, 1667, 1600, 1531, 1439, 1116. HRMS ESI:  $(\text{M} + \text{Na})^+$   $\text{C}_{23}\text{H}_{25}\text{N}_3\text{O}_3\text{Na}$  calcd 414.17936, found 414.1777.

**Acknowledgment.** We thank MENRT, CNRS, and La Ligue Contre le Cancer, Comité de Charente-Maritime for financial support. G.E. and O.W. thank the Walther Cancer Institute at the University of Notre Dame for continued financial support.

**Supporting Information Available:** Experimental details for the synthesis of compounds **9**, **10b**, **13a,b**, **16a,b**, **18a,b**, and **19a,b**, the analytical and spectral data for all compounds, the biological evaluations of compounds **7a–d**, and the molecular modeling methods. This material is available free of charge via the Internet at <http://pubs.acs.org>.

## References

- (1) (a) Baylin, S. B.; Ohm, J. E. Epigenetic gene silencing in cancer—a mechanism for early oncogenic pathway addiction. *Nat. Rev. Cancer* **2006**, *6*, 107. (b) Xu, W. S.; Parmigiani, R. B.; Marks, P. A. Histone

deacetylase inhibitors: molecular mechanisms of action. *Oncogene* **2007**, *26*, 5541.

- (2) Hodawadekar, S. C.; Marmorstein, R. Chemistry of acetyl transfer by histone modifying enzymes: structure, mechanism and implications for effector design. *Oncogene* **2007**, *26*, 5528.
- (3) Dokmanovic, M.; Clarke, C.; Marks, P. A. Histone deacetylase inhibitors: overview and perspectives. *Mol. Cancer Res.* **2007**, *5*, 981.
- (4) Duvic, M.; Talpur, R.; Ni, X.; Zhang, C.; Hazarika, P.; Kelly, C.; Chiao, J. H.; Reilly, J. F.; Ricker, J. L.; Richon, V. M.; Frankel, S. R. Phase 2 trial of oral vorinostat (suberoylanilide hydroxamic acid, SAHA) for refractory cutaneous T-cell lymphoma (CTCL). *Blood* **2007**, *109*, 31.
- (5) (a) Finnin, M. S.; Donigan, J. R.; Cohen, A.; Richon, V. M.; Rifkind, R. A.; Marks, P. A.; Breslow, R.; Pavletich, N. P. Structures of a histone deacetylase homologue bound to the TSA and SAHA inhibitors. *Nature (London)* **1999**, *401*, 188. (b) Somoza, J. R.; Skene, R. J.; Katz, B. A.; Mol, C.; Ho, J. D.; Jennings, A. J.; Luong, C.; Arvai, A.; Buggy, J. J.; Chi, E.; Tang, J.; Sang, B. C.; Verner, E.; Wynands, R.; Leahy, E. M.; Dougan, D. R.; Snell, G.; Navre, M.; Knuth, M. W.; Swanson, R. V.; McRee, D. E.; Tari, L. W. Structural snapshots of human HDAC8 provide insights into the class I histone deacetylases. *Structure* **2004**, *12*, 1325.
- (6) Vannini, A.; Volpari, C.; Gallinari, P.; Jones, P.; Mattu, M.; Carfi, A.; De Francesco, R.; Steinkühler, C.; Di Marco, S. Substrate binding to histone deacetylases as shown by the crystal structure of the HDAC8–substrate complex. *EMBO Rep.* **2007**, *8*, 879.
- (7) Nielsen, T. K.; Hildmann, C.; Dickmanns, A.; Schwienhorst, A.; Ficner, R. Crystal structure of a bacterial class 2 histone deacetylase homologue. *J. Mol. Biol.* **2005**, *354*, 107.
- (8) Khan, N.; Jeffers, M.; Kumar, S.; Hackett, C.; Boldog, F.; Khramtsov, N.; Qian, X.; Mills, E.; Berghs, S. C.; Carey, N.; Finn, P. W.; Collins, L. S.; Tumber, A.; Ritchie, J. W.; Jensen, P. B.; Lichenstein, H. S.; Sehested, M. Determination of the class and isoform selectivity of small-molecule histone deacetylase inhibitors. *Biochem. J.* **2008**, *409*, 581.
- (9) KrennHrubic, K.; Marshall, B. L.; Hedglin, M.; Verdin, E.; Ulrich, S. M. Design and Evaluation of “Linkerness” Hydroxamic Acids as Selective HDAC8 Inhibitors. *Bioorg. Med. Chem. Lett.* **2007**, *17*, 2874.
- (10) (a) Kozikowski, A. P.; Tapadar, S.; Luchini, D. N.; Kim, K. H.; Billadeau, D. D. Use of the Nitrile Oxide Cycloaddition (NOC) Reaction for Molecular Probe Generation: A New Class of Enzyme Selective Histone Deacetylase Inhibitors (HDACi) Showing Picomolar Activity at HDAC6. *J. Med. Chem.* **2008**, *51*, 4370–4373. (b) Estiu, G.; Greenberg, E.; Harrison, C. B.; Kwiatkowski, N. P.; Mazitschek, R.; Bradner, J. E.; Wiest, O. Structural Origin of Selectivity in Class II-Selective Histone Deacetylase Inhibitors. *J. Med. Chem.* **2008**, *51*, 2898–2906.
- (11) (a) Weerasinghe, S. V. W.; Estiu, G.; Wiest, O.; Pflum, M. K. H. Residues in the 11 Å Channel of Histone Deacetylase 1 Promote Catalytic Activity: Implications for Designing Isoform-Selective Histone Deacetylase Inhibitors. *J. Med. Chem.* **2008**, *51*, 5542–5551. (b) Witter, D.; Belvedere, S.; Chen, L.; Secrist, J.; Mosley, R.; Miller, T. A. Benzo[*b*]thiophene-based histone deacetylase inhibitors. *Bioorg. Med. Chem. Lett.* **2007**, *17*, 4562–4567.
- (12) (a) Charrier, C.; Bertrand, P.; Gesson, J.-P.; Roche, J. Synthesis of rigid trichostatin A analogs as HDAC inhibitors. *Bioorg. Med. Chem. Lett.* **2006**, *16*, 5339. (b) Charrier, C.; Roche, J.; Gesson, J.-P.; Bertrand, P. Antiproliferative activities of a library of hybrids between indanones and HDAC inhibitor SAHA and MS-275 analogues. *Bioorg. Med. Chem. Lett.* **2007**, *17*, 6142.
- (13) Ohira, T.; Gemmill, R.; Ferguson, K.; Kusy, S.; Roche, J.; Brambilla, E.; Zeng, C.; Baron, A.; Bemis, L.; Erickson, P.; Wilder, E.; Rustgi, A.; Kitajewski, J.; Gabrielson, E.; Bremnes, R.; Franklin, W.; Drabkin, H. WNT7a induces E-Cadherin in lung cancer cells. *Proc. Natl. Acad. Sci. U.S.A.* **2003**, *100*, 10429.
- (14) Potiron, V.; Roche, J.; Drabkin, H. Semaphorins and their receptors in lung cancer. *Cancer Lett.* **2009**, *273*, 1.

JM9002439